Reflective Properties of Natural Snow: Approximate Asymptotic Theory Versus *In Situ* Measurements

Alexander A. Kokhanovsky, Teruo Aoki, Akihiro Hachikubo, Masahiro Hori, and Eleonora P. Zege

***Abstract*—Results of measurements of the bidirectional reflection function of snow for the solar zenith angle close to 54° are compared with a recently developed snow optical model based on the representation of snow grains as fractal particles. The model has a high accuracy out of the principal plane for the observation zenith angles smaller than 60°. However, the accuracy is reduced in the principal plane. Specular light reflection by partially oriented snow plates on the snow surface not accounted for by the model can play a role for measurements in the principal plane. The model discussed can be used for the grain size retrieval using both ground and spaceborne measurements of the snow reflectance. This is supported by a high accuracy of the model in a broad spectral range 545–2120 nm as demonstrated in this work.**

***Index Terms*—Light reflectance, light scattering, radiative transfer, remote sensing, snow.**

I. Introduction

POLAR areas are covered by ice and snow. Also, snow covers great portions of Eurasia and Nothern America in winter months, changing the planetary albedo. It has been argued that the snow albedo is modified by an anthropogenic interference [4].

In particular, the average concentration of soot in the Arctic has been increased almost eight times during the time period 1983–1998 [4]. Such findings are of a great importance and should be confirmed by independent measurements especially those involving data from orbiting satellites.

Aoki *et al.* [3] showed that the snow grain size d and the concentration c of impurities in snow are very important factors for the snow albedo r. Both c and d have been retrieved from satellite data using the algorithm in which snow grains are assumed to be spherical [5].

To decode the information contained in the spectral signatures of snow as detected from a satellite, a comprehensive theory of snow optical properties is needed. This is an extremely complex task due to the complex internal structure of snow [13], [16]. The horizontal and vertical inhomogeneity of snow (e.g., snow layers deposited at different times) add even more complexity to the problem.

The main task of this paper is to validate an approximate asymptotic theory (AAT) of snow optical properties developed elsewhere [10] using *in situ* measurements of snow reflectance in visible and near-infrared. In particular, measurements at the wavelengths 545, 1050, 1240, and 2210 nm have been compared with the AAT. They coincide with atmospheric windows, where gaseous absorption can be neglected or easily taken into account. Correspondent measurements have been performed in Hokkaido, Japan on February 9, 2001. The AAT is valid only for optically thick weakly absorbing snow layers. Therefore, the case of extremely dirty snow cannot be considered in the framework of the AAT.

The results of this work can be used for monitoring of snowpack properties (e.g., the ice grain size and the concentration of pollutants) using satellite measurements.

II. Theory

The snow reflection function can be modeled using the following approximate analytical solution of this equation valid in the limit of small light absorption by snow grains [10]

$$R(\vec{q}) = R_0(\vec{q}) \exp\left(-\alpha f(\vec{q})\right). \tag{1}$$

Here R is the bidirectional reflectance (or the reflection function) of a semi-infinite snow layer. The vector-parameter $\vec{q}$ has coordinates ϑ_0, ϑ, φ, which are the incidence zenith angle, the observation zenith angle, and the relative azimuth, respectively.

The function $f(\vec{q})$ in (1) is given by the following ratio:

$$f(\vec{q}) = \frac{K_0(\vartheta_0)K_0(\vartheta)}{R_0(\vartheta_0, \vartheta, \varphi)} \tag{2}$$

where R_0 equals to the value of R at zero absorption and

$$K_0(\vartheta_0) = \frac{3}{4}\cos\vartheta_0 + \frac{3}{4\pi}\int_0^{2\pi} d\varphi \int_0^{\frac{\pi}{2}} R_0(\vartheta_0, \vartheta, \varphi)\cos^2\vartheta \sin\vartheta d\vartheta. \tag{3}$$

The function $K_0(\vartheta_0)$ is called the escape function in radiative transfer theory. It determines the angular distribution of light escaping the semi-infinite nonabsorbing medium in the framework of the Milne problem (with sources located at infinity inside a

Manuscript received June 9, 2004; revised March 6, 2005. This work was supported in part by the Deutschen Forschungsgemeinschaft (DFG) Project BU 688/8-1 and in part by the Japan Aerospace Exploration Agency under Contract G-0054. The fieldwork was conducted as part of the ADEOS II/GLI Cal/Val experiment supported by the Japan Aerospace Exploration Agency.

A. A. Kokhanovsky is with the Institute of Environmental Physics, Bremen University, D-28213 Bremen, Germany, and also with the B. I. Stepanov Institute of Physics, National Academy of Sciences of Belarus, 220072 Minsk, Belarus (e-mail: alexk@iup.physik.uni-bremen.de).

T. Aoki is with the Meteorological Research Institute, Tsukuba, 305-0052 Ibaraki, Japan.

A. Hachikubo is with the Kiami Institute of Technology, New Energy Resources Center, Kitami Institute of Technology, 090-8507 Kitami, Japan.

M. Hori is with the Earth Observation Research and Application Center, Japan Aerospace Exploration Agency, 104-6023 Tokyo, Japan.

E. P. Zege is with the B. I. Stepanov Institute of Physics, National Academy of Sciences of Belarus, 220072 Minsk, Belarus.

Digital Object Identifier 10.1109/TGRS.2005.848414

medium). It can be approximated by the following equation [9] at $\xi \geq 0.2$:

$$K_0(\xi) = \frac{3}{7}(1 + 2\xi) \tag{4}$$

where $\xi = \cos\vartheta_0$. The approximation (4) contributes to biases of the ATT as compared to experiments for angles larger than approximately 75°. However, the error of (4) is below 2% for smaller angles.

The value of α is given by the following equation:

$$\alpha = 4\sqrt{\frac{l_{tr}}{3l_{abs}}} \tag{5}$$

where l_{abs} is the absorption path length and l_{tr} is the transport path length. Studies of the accuracy of (1) as compared to the solution of the radiative transfer equation have been conducted by Kokhanovsky [6], [7]. It was found that (1) can be applied for the values of α smaller than approximately 1.5.

Kokhanovsky and Zege [10] derived the following relationship for the value of α in the framework of the approximation of fractal snow grains:

$$\alpha = B\sqrt{\gamma d} \tag{6}$$

where $\gamma = 4\pi\chi/\lambda$, χ is the imaginary part of the refractive index of ice, $d = 6\langle V\rangle/\langle S\rangle$ is the effective grain size, and $B \approx 3.6$. Here $\langle V\rangle$ is the average volume of grains and $\langle S\rangle$ is their average surface area. Clearly, we have for monoidispersed spherical grains with the radius a: $d = 2a$. So d has the meaning of a diameter for spheres.

Combining all equations given above it is possible to arrive to the following parameterization of the snow spectral reflection function:

$$R(\vartheta_0, \vartheta, \varphi) = R_0(\vartheta_0, \vartheta, \varphi)\exp(-A\sqrt{\gamma d}) \tag{7}$$

where

$$A = \frac{0.66(1 + \cos\vartheta_0)(1 + \cos\vartheta)}{R_0(\vartheta_0, \vartheta, \varphi)}. \tag{8}$$

The constant A is determined by the observation geometry and local scattering characteristics of snow. Its dependence on the grain size, the wavelength, and the absorption coefficient can be neglected. The product $c = \gamma d$ determines the attenuation of the optical wave on the grain effective diameter (e.g., it follows for the transmitted light intensity: $I = I_0\exp(-c)$, where I_0 is the incident light intensity at the surface of the grain).

Therefore, the snow reflection function is parameterised in terms of the diameter d, the reflection function of a semi-infinite snow layer at zero absorption $R_0(\vartheta_0, \vartheta, \varphi)$, and the angular factor A, which accounts for the influence of geometry on the level of light absorption by snow.

Clearly, the absorption of light by snow should be larger for the illumination along normal to a snow layer, and this is accounted for by the angular factor A.

Fig. 1. Photo of the measurement site in Hokkaido.

III. Reflection Function of Snow

A. Experimental Setup

Measurements of snow reflection functions were made on February 9, 2001 (12:00, local time) at Bihoro in eastern Hokkaido close to the measurement site described by Aoki *et al.* [2]. The photo of the site is given in Fig. 1. This photo was taken not during measurements but at a different day.

There were no clouds and air temperatures were below −10 °C during measurements. The snow depth was 41 cm. The snow surface was covered by a thin layer of fresh snow with the depth of 2 mm. Most of crystals were dendrites. The snow layers to the depth of 7 cm consisted of fine-grained old snow and faceted crystals, and the layers from 7 cm to the bottom were depth hoar and ice layers.

Snow grain sizes (radii) were estimated *in situ* using a handheld lens together with micrographs. This measurement gave three kinds of dimensions of grains; one was a half the length of the major axis of crystals or dendrites (r_1) and the second was a half the branch width of dendrites (HBWD) or a half the dimension of narrower portion of broken crystals (r_2), and the third was a snow crystal thickness (r_3). We found that $r_1 = 0.1-1.0$ mm, $r_2 = 0.03-0.15$ mm, and $r_3 = 0.01-0.02$ mm. Aoki *et al.* [1], [2] concluded that optically equivalent snow grain size was r_2 from the comparison of measured spectral albedo with theoretically calculated ones. This means that the value of d defined in the previous section must be in the range 0.06–0.3 mm for the upper layer of snow.

We find (see below) that the value of $r = 0.06$ mm ($d = 0.12$ mm) must be used to fit measurements using our theory. This value falls in the range of measured r_2. It confirms the finding of Aoki *et al.* [1], [2] that the optical equivalent snow grain size is not r_1 or r_3, but r_2 (HBWD).

Our measurements have shown that the snow was contaminated by dust particles and, probably, by other impurities including soot. The contamination was found both at 0–1 cm and 1–10 cm depths. The newly fallen snow was polluted by dirty snow deposited at lower layers. The total mass concentrations of impurities was measured and found to be equal to 3.7 ppmw.

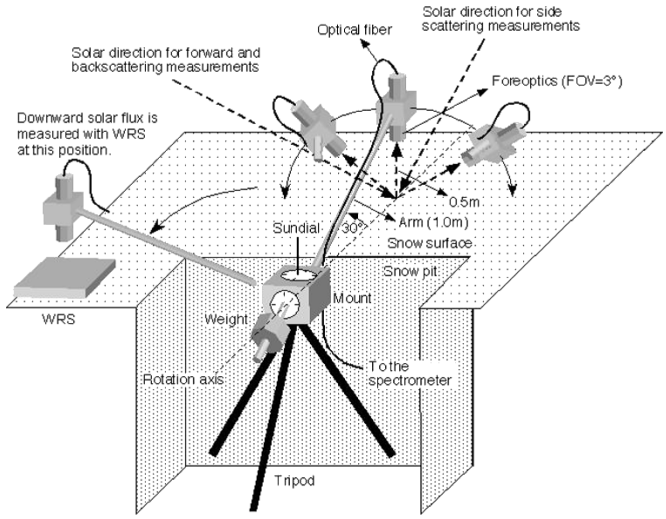

Fig. 2. Measurement system.

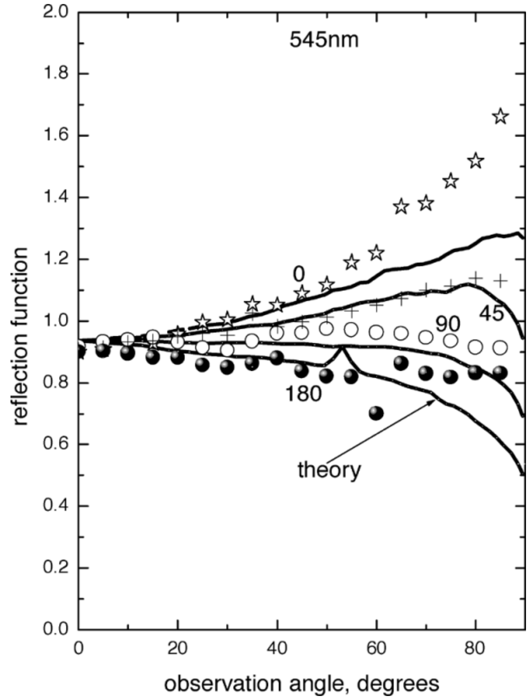

Fig. 3. Dependence of snow reflection function on the observation zenith angle (symbols-measurements for azimuths equal to 0°, 45°, 90°, 180°, lines-numerical calculations for the same azimuths at the wavelength 545 nm. The sun angle was in the range 53.5° to 54.6° during measurements. Measurements were taken out at the zenith observation angles equal to 0°, 10°, 20°, 30°, 40°, 50°, 60°, 70°, 80°, and 85°.

We did not incorporate the influence of the impurities in the theoretical model because their influence is of importance only in visible. Moreover, the refractive index of impurities is not well characterized.

The instruments used for the measurements consist of the spectrometer and the pointing system for snow surface.

The former is a grating spectrometer, "FieldSpec FR," made by ASD Inc. (Boulder, CO), which is the same as that used by Aoki *et al.* [2]. The scanning spectral range of this instrument was 0.35–2.5 μm with the spectral resolution of 3 nm for $\lambda = 0.35 - 1.0$ μm and 10 nm for $\lambda = 1.0 - 2.5$ μm. The scanning time is 1 s with a sampling interval of 1 nm for the full spectral range. The detectors are one-dimensional Si photodiode CCDs for $\lambda = 0.35 - 1.0$ μm and two different types of InGaAs photodiodes for $\lambda = 1.0 - 1.8$ μm and $\lambda = 1.8 - 2.5$ μm.

The pointing system is the system to observe the same snow surface from any viewing angle (see Fig. 2). The reflected light from snow surface is taken into spectrometer by foreoptics with the field of view (FOV) equal to 3° and by the optical fiber. The foreoptics is connected to the arm which has an angle of 30° from the rotation axis in the mount, where the rotation axis in the mount is set at the same level as snow surface using the elevator of tripod. The foreoptics can observe the same snow surface from different viewing angles by rotating the arm as shown in Fig. 2. The azimuth direction of the bidirectional reflectance to be measured is tuneable by changing the azimuth direction of the apparatus relative to the sun, where sundial is used to detect the solar direction. The downward radiant flux, which is necessary to get the reflectance, is measured by using white reference standard (WRS) shown in Fig. 2. The solar zenith angle was in the range from 53.5° to 54.6° during measurements.

Although the foreoptics points the same snow surface from any viewing angle, the precise area of the measured snow surface varies with the viewing angle. The area of measurements is circular for the nadir observations. It changes to an ellipse for nonnadir observation geometries. However, the smoother reflection functions could be obtained with this system compared with the optical system used by Aoki *et al.* [2].

B. Comparison of Theoretical and Experimental Results

1) Visible Range: The measured snow reflection function at the wavelength 545 nm is given in Fig. 3 for the relative azimuths 0°, 45°, 90°, and 180° (symbols). The azimuth 0° corresponds to the forward scattering in the principal plane. At this azimuth, the specular Fresnel reflection from the snow crust can appear at solar zenith angles equal to the observation angle. There were no crust at the snow surface during measurements as it was specified in the previous section.

Because $\gamma d \approx 0$ at this wavelength, it follows: $R(\vartheta_0, \vartheta, \varphi) \approx R_0(\vartheta_0, \vartheta, \varphi)$. The function $R_0(\vartheta_0, \vartheta, \varphi)$ has been calculated solving the nonlinear integral transport equation (NITE) as described by Mishchenko *et al.* [14]. It was assumed that the single-scattering albedo is equal to one and the phase function is calculated in the assumption of the fractal snow grains (see Macke *et al.* [12] and Mishchenko *et al.* [14] for details) with the value of d equal to 0.12 mm. Due to the absence of absorption and the large size of grains $(d \gg \lambda)$, the snow phase function does not depend on the value of d (at least outside of the small diffraction region, which is of no interest as far as light reflection is concerned). Further details on the snow particle model used in this paper are given by Macke *et al.* [12], Mishchenko *et al.* [14], Kokhanovsky [8], and Kokhanovsky and Zege [10].

The results of numerical calculations for a semi-infinite snow layer are given in Fig. 3 by lines. The semi-infinite layer approximation can be used because of large geometrical thickness of snow as described in the previous section. Note that all theoretical curves were normalized to one value $(R = 0.94)$ obtained

from measurements at the observation angle equal to 0° and for the solar zenith angle equal to 54°. The theory gives $R = 1.0$ in this case, which is by 6% higher than results obtained from the experiment for this particular case. This difference could be explained by the impurities in snow (e.g., soot and dust).

Data given in Fig. 3 make it possible to make the following conclusions.

- The radiative transfer equation is capable to predict the decrease of the reflection function with the azimuth φ as found in the experiment. This is mostly due to the decrease of the scattering angle θ and, correspondingly, the increase of the phase function with φ in cases considered.
- The accuracy is high at azimuths 45° and 90°.
- The errors of the approximation are small at observation angles smaller than 60° for all azimuths studied.
- The accuracy decreases for the large observation angles both for forward scattering (0°) and backward scattering (180°). In both cases the radiative transfer equation underestimates the snow reflection. Most probably this is due to the specular reflection from the surface of partially oriented plate-like crystals positioned in the upper layer of snow. The effect is easily observed as a diamond-like shining of a newly fallen snow. So the additional component should be added to the value of R given by (7). However, such large observation angles are not used in snow remote sensing. So we do not modify our model to account for possible large values of the solar zenith angle.

Summing up, we conclude that NITE gives an accurate approximation for the bidirectional snow reflectance in visible (e.g., for the snow satellite remote sensing purposes). Large discrepancy of measurements and the theory for the relative azimuth 0° and observation angles larger than 60° is not related to errors of the AAT as compared to the integro-differential radiative transfer equation [14] but rather it is due to conceptual problems of the forward model used.

Indeed, it follows from the experiment that the reflection function is close to 1.5 at the observation angle 80° and even higher for the observation zenith angle 85° (see Fig. 3). Such large values of R cannot be described in the framework of the standard radiative transfer equation for plane-parallel layers [14]. We remind that R gives the ratio of the reflected light intensity I to the value of I, if the snow surface is substituted by a Lambertian absolutely white surface. Most probably, three-dimensional effects and also the specular reflection component must be taken into account to increase the accuracy for large zenith observation angles in the principal plane.

2) Near-Infrared Range: Theoretical curves $R(\vartheta) \approx R_0(\vartheta)$ given in Fig. 3 have been used [in conjunction with (7) at $d = 0.12$ mm] to model the reflection function of snow at several wavelengths as is shown in Figs. 4 and 5 for azimuths 45° and 90°, solar zenith angle 54°, and zenith observation angles 0°, 10°, 20°, 30°, 40°, 50°, 60°, 70°, 80°, and 85°.

The value of d is a free parameter of our theory. So it was selected to be equal 0.12 mm to have a best fit of our theory with respect to measured results. Note that the value of d falls in the range of the crystal size variability during measurements (see Section III-A).

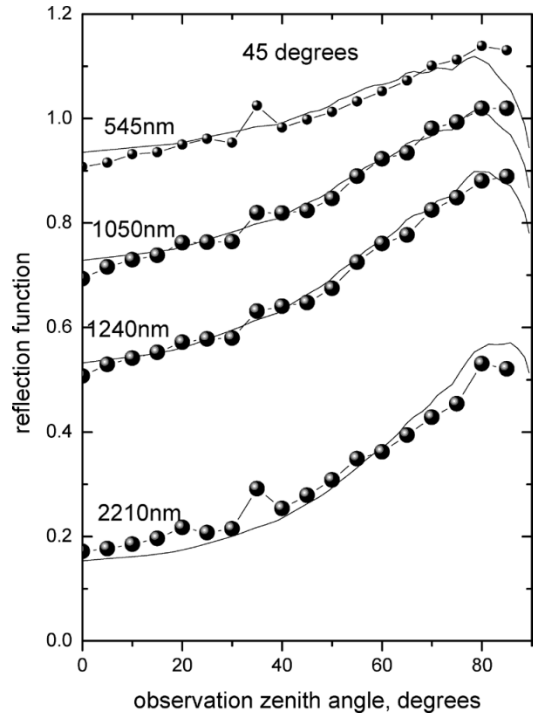

Fig. 4. Dependence of the snow reflection function on the observation zenith angle (symbols-measurements at the azimuth equal to 45°, lines-numerical calculations) at the wavelengths 545, 1050, 1240, 2210 nm and $d = 0.12$ mm. The values of χ have been taken from data given by Warren [17]. The illumination/viewing geometry is the same as in Fig. 3.

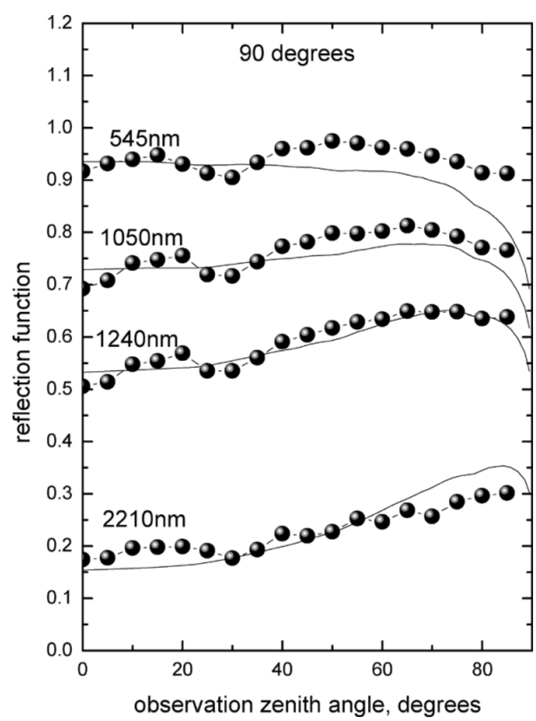

Fig. 5. Same as in Fig. 4 except at the azimuth $\varphi = 90°$.

It follows from Figs. 4 and 5 that the exponential factor in (7) describes the behavior of experimental curves at azimuths 45° and 90° for almost all observation angles in the broad spectral range 545–2210 nm with a high accuracy at $d = 0.12$ mm. The accuracy is poor at observation angles larger than 60° in the

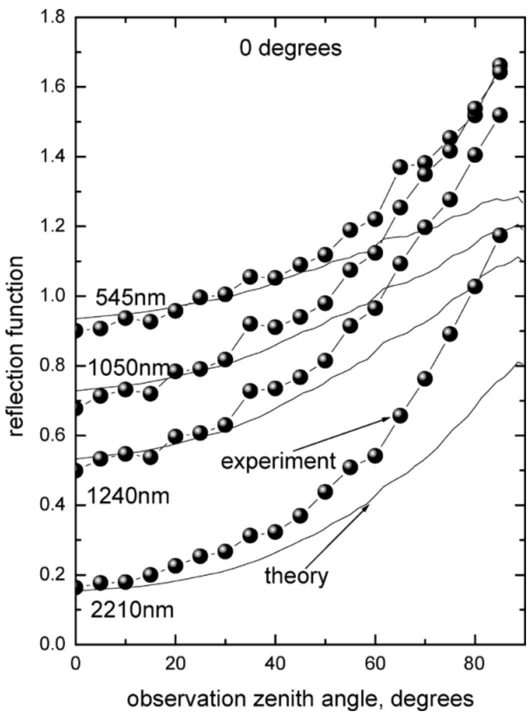

Fig. 6. Same as in Fig. 4 except at the azimuth $\varphi = 0°$.

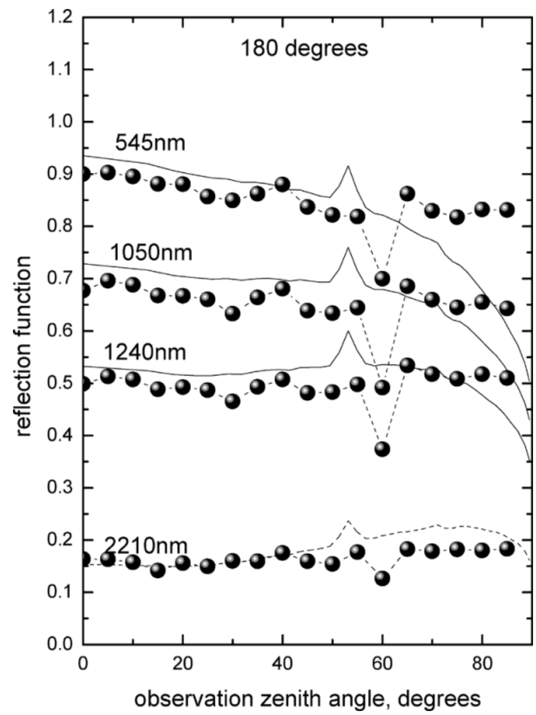

Fig. 7. Same as in Fig. 4 except at the azimuth $\varphi = 180°$.

principal plane (see Figs. 6 and 7). The principal plane contains the Sun, normal to the snow surface and the observation direction (the azimuth equals to 0° for forward scattering and the azimuth equals to 180° for backward scattering). This is mostly due to the usage of theoretical reflection functions shown in Fig. 3. These functions are not accurate enough in the principal plane at large observation angles. The accuracy can be considerably increased (not shown here), if the experimental reflection functions shown in Fig. 3 are used in (7) to simulate near-infrared observations. This underlines the fact that the exponential factor in (7) captures the physics of the problem in a correct way.

Both the experiment and the theory point out to the fact that the dependence of the light reflection on the observation angle is stronger for wavelengths, where light absorption is somewhat larger. For instance, the slope of R as the function of the observation angle in Fig. 4 strongly depends on the level of light absorption by snow grains, which is larger for larger wavelengths. The accuracy of angular and spectral fits as shown in Fig. 4 is quite remarkable taking into account the simplicity of (7) and the complexity of light transport in snow.

Figs. 3–7 confirm that snow cannot be described by a Lambertian surface model. Then, it follows by definition that $R = const$. This is clearly not the case as indicated in Figs. 3–7. The deviations from a Lambertian surface model generally grow with the wavelength.

Minima in experimental curves around the observation angle equal 30° in Fig. 5 (and, probably, also maxima around 35° in Fig. 4) may be explained by the fact that the snow layer was not ideally plane parallel medium as it is assumed in the theoretical model. So these oscillations of experimental curves are best explained by the undulation of the snow surface not accounted for in the model. The difference in the reflection functions for azimuths φ and $\varphi + \pi$ observed in the experiment (not shown here) also points in this direction. Actually, the correspondence of the theory and experiment could be made even better if we use as the experimental value not $R(\varphi)$ but $\overline{R}(\varphi) = 0.5(R(\varphi) + R(\varphi + \pi))$. Then both experimental errors and the inhomogeneity of the surface effects are largely reduced.

The peaks close to 50° seen in theoretical curves in Fig. 7 are not observed in experimental data at $\varphi = 180°$. These peaks originate from the peak of the phase function $p(\theta)$ of fractal particles in the exactly backward direction. This peak is most probably due to the inaccuracy of geometrical optics calculations for fractal particles at $\theta = 180°$. So in future for modeling snow optical properties the snow phase function obtained in the fractal model [12] should be used only for values of $\theta \leq 175°$. Then one can assume $p(\theta) = p(175°)$ at $\theta \in [175°, 180°]$.

The minima in experimental data around 60° (see Fig. 7) are due to a shadow caused by the instrument.

IV. Optical Sizing of Snow Grains

We see that (7) can be used to model snow reflection function in visible and near-infrared with exclusion of large observation angles in the principal plane. This is mostly is due to the fact that α is below 1.5 for measurements at wavelengths 545 nm ($\alpha \approx 0.01$), 1050 nm ($\alpha \approx 0.19$), 1240 nm ($\alpha \approx 0.43$), 2210 nm ($\alpha \approx 1.40$) reported here. A high accuracy of the AAT as found in this work in a broad spectral range opens up a simple way of the determination of the grain size from the measured reflection function R by ground-based or orbiting optical instruments.

In particular, it follows from (7)

$$d = \frac{1}{A^2\gamma} \ln^2\left(\frac{R}{R_0}\right). \tag{9}$$

It should be emphasized that all parameters in (9) (except R_0) are given by simple analytical formulae specified above. This allows for the determination of d from the measured value of R if R_0 is obtained from precalculated lookup tables for fractal particles. Note that R_0 is close to one for fractal particles at the nadir observation [10]. If a high accuracy is not of a primary importance, then the following parameterization for R_0 can be used [11]:

$$R_0(\vartheta_0, \vartheta, \varphi) = \frac{A + B(\xi + \eta) + C\xi\eta + p(\theta)}{4(\xi + \eta)} \tag{10}$$

where

$$A = 1.247 \quad B = 1.186 \quad C = 5.157 \tag{11}$$

$p(\theta)$ is the phase function and

$$\theta = \cos^{-1}\left(-\xi\eta + \sqrt{(1-\xi^2)(1-\eta^2)}\cos\varphi\right) \tag{12}$$

is the scattering angle, and $\xi = \cos\vartheta_0$, $\eta = \cos\vartheta$. The calculation of $p(\theta)$ for irregularly shaped ice crystals requires long computation time. Therefore, the following parameterization has been developed [11]:

$$p(\theta) = 11.1\exp(-0.087\theta) + 1.1\exp(-0.014\theta) \tag{13}$$

where $\theta \geq 10^\circ$ is expressed in degrees. The accuracy of (10) is better than 3% for the nadir observation and incidence angles smaller than 78°. The error is below 10% at $\xi \geq 0.2$, $\eta \geq 0.9$.

If the value of d is obtained from measurements in the near infrared (e.g., at 1240 nm), then measurements in visible (e.g., at 545 nm) can be used to deduce the snow absorption coefficient γ_{vis}. Namely, it follows from (9)

$$\gamma_{vis} = \frac{1}{A^2 d}\ln^2\left(\frac{R}{R_0}\right). \tag{14}$$

Clearly, γ_{vis} should correlate with the soot concentration c (and, possibly, with abundances of other absorbers) as discussed by Zege *et al.* [15]. This allows for the development of techniques to monitor the contamination of snow fields by soot from space.

V. Conclusion

The asymptotic radiative transfer theory as applied to the snow reflection function calculation [10] has been used for the interpretation of *in situ* measurements performed in Hokkaido, Japan on February 9, 2001. A close correspondence of theory and experimental results is found outside of the principal plane using the effective grain size $d = 0.12$ mm. This means that we also retrieved the optically equivalent size of snow grains by comparing our measurements with the theory. The value of d falls in the range of measured lengths of the branch width of dendrites or dimensions of narrower portions of broken crystals. This confirms similar findings of Aoki *et al.* [1], [2]. More measurements are needed to establish the correlation between the optically equivalent radius as retrieved from the reflectance measurements with actual sizes of grains as measured *in situ*.

In the principal plane, which holds the observation and illumination directions, the accuracy of the approximation is low for large observation angles. This can be attributed to effects of the specular light reflections by tiny ice crystals deposited on the snow surface. These reflections are not accounted in the model considered here.

We underline that only a small subset of measurements performed was analyzed in this work. However, we found that the subset used captures the major angular characteristics of the snow reflectance.

Results obtained show that our theory [see (7)] can be used to monitor the grain size and also the level of snow pollution from spaceborne optical instrumentation. For this, however, the atmospheric correction of snow imagery should be performed, which is not an easy task taking into account problems with the aerosol optical thickness retrieval over bright surfaces. However, this is a crucial point only in visible. The snow is almost black in near-infrared (see Figs. 4–7). This makes retrieval of the aerosol properties over snow in near-infrared much more simple than this is the case in the visible.

Other urgent point to be addressed is the relation of the retrieved optically equivalent ice grain size to that measured *in situ*. For this, however, dedicated campaigns with much more advanced techniques as compared to those used in this study for *in situ* ice grains particle sizing must be utilized (e.g., in conjunction with spectral reflectance measurements). In particular, the automatic image analysis techniques look very promising in this respect.

Acknowledgment

The authors are grateful to M. I. Mishchenko for providing the computer code used in this paper and also to A. Macke and T. Nakajima for important discussions.

References

[1] T. Aoki, T. Aoki, M. Fukabori, Y. Tachibana, F. Nishio, and T. Oishi, "Spectral albedo observation of the snow field at Barrow," *Polar Meteorol. Glaciol.*, vol. 12, pp. 1–9, 1998.
[2] T. Aoki, T. Aoki, M. Fukabori, A. Hachikubo, Y. Tachibana, and F. Nishio, "Effects of snow physical parameters on spectral albedo and bi-directional reflectance of snow surface," *J. Geophys. Res.*, vol. 105, pp. 10 219–10 236, 2000.
[3] T. Aoki, A. Hachikubo, and M. Hori, "Effects of snow physical parameters on broad-band albedos," *J. Geophys. Res.*, vol. 108, p. 4616, 2003. DOI: 10.1029/2003JD003506.
[4] J. Hansen and L. Nazarenko, "Soot climate forcing via snow and ice albedos," *Proc. Nat. Acad. Sci.*, vol. 101, pp. 423–428, 2004.
[5] M. Hori, T. Aoki, K. Stamnes, B. Chen, and W. Li, "Preliminary validation of the GLI algorithms with MODIS daytime data," *Polar Meteorol. Glaciol.*, vol. 15, pp. 1–20, 2001.
[6] A. A. Kokhanovsky, "Reflection and polarization of light by semi-infinite turbid media: Simple approximations," *J. Col. Interf. Sci.*, vol. 251, pp. 429–431, 2002a.
[7] ——, "The accuracy of selected approximations for the reflection function of a semi-infinite turbid medium," *J. Appl. Phys. D*, vol. 35, pp. 1057–1062, 2002b.
[8] ——, "Optical properties of irregularly shaped particles," *J. Appl. Phys. D*, vol. 36, pp. 915–923, 2003.
[9] A. A. Kokhanovsky, V. V. Rozanov, E. P. Zege, H. Bovensmann, and J. P. Burrows, "A semi-analytical cloud retrieval algorithm using backscattering radiation in 04.–2.4 μm spectral range," *J. Geophys. Res. D*, vol. 108, 2003. DOI: 10.1029/2001JD001543.

[10] A. A. Kokhanovsky and E. P. Zege, "Scattering optics of snow," *Appl. Opt.*, vol. 43, pp. 1589–1602, 2004.

[11] A. A. Kokhanovsky, "Reflection of light from a semi-infinite medium with irregularly shaped particles," *J. Quant. Spectrosc. Radiat. Transf.*, vol. 96, pp. 1–10, 2005.

[12] A. Macke, J. Mueller, and E. Raschke, "Scattering properties of atmospheric ice crystals," *J. Atmos. Sci.*, vol. 53, pp. 2813–2825, 1996.

[13] R. A. Massom, H. Eicken, C. Haas, M. O. Jeffris, M. R. Drinkwater, M. Sturm, A. P. Worby, X. Wu, V. I. Lytle, S. Ushio, K. Morris, P. A. Reid, S. G. Warren, and I. Allison, "Snow on Antarctic ice," *Rev. Geophys.*, vol. 39, pp. 413–445, 2001.

[14] M. I. Mishchenko, J. M. Dlugach, E. G. Yanovitskij, and N. T. Zakharova, "Bidirectional reflectance of flat, optically thick particulate layers: An efficient radiative transfer solution and applications to snow and soil surfaces," *J. Quant. Spectrosc. Radiat. Transf.*, vol. 63, pp. 409–432, 1999.

[15] E. P. Zege, A. A. Kokhanovsky, I. L. Katsev, I. N. Polonsky, and A. S. Prikhach, "The retrieval of the effective radius of snow grains and control of snow pollution with GLI data," in *Proc. Conf. Light Scattering by Nonspherical Particles: Theory, Measurements, and Applications*, M. I. Mishchenko, L. D. Travis, and J. W. Hovenier, Eds., Boston, MA, 1998, pp. 288–290.

[16] S. G. Warren, "Optical properties of snow," *Rev. Geophys. Space Sci.*, vol. 2, pp. 67–89, 1982.

[17] ——, "Optical constants of ice from the ultraviolet to the microwave," *Appl. Opt.*, vol. 23, pp. 1206–1225, 1984.

Alexander A. Kokhanovsky received the M.S. degree in theoretical physics from the Belarussian State University, Minsk, Belarus, in 1983, and the Ph.D. degree in optical sciences from the B.I. Stepanov Institute of Physics, National Academy of Sciences of Belarus, Minsk, in 1991. His Ph.D. work was devoted to modeling light scattering properties of various aerosol media and foams.

He is currently a member of the SCIAMACHY/ENVISAT algorithm development team at the Institute of Environmental Physics, University of Bremen, Bremen, Germany. His research interests are directed toward modeling light propagation and scattering in terrestrial atmosphere. He is the author of the books *Light Scattering Media Optics: Problems and Solutions* (Chichester, U.K.: Springer-Praxis, 1999, 2001, 2004) and *Polarization Optics of Random Media* (Berlin, Germany: Springer-Praxis, 2003). He has published more than 70 papers in the field of environmental optics, radiative transfer, and light scattering.

Dr. Kokhanovsky is a member of the American Geophysical Union and the Belarussian Physical Society.

Teruo Aoki received the B.S. degree in meteorology from the Meteorological College, Kashiwa, Japan, in 1981, and the Ph.D. degree in polar science from the National Institute of Polar Research (The Graduate University of Advanced Studies), Tokyo, Japan.

He is currently a Senior Researcher at the Meteorological Research Institute of the Japan Meteorological Agency, Ibaraki. His research interests are optical properties of snow and satellite remote sensing in cryosphere. He performs experiments in Japan, Alaska, Antarctica, and the Himalayas.

Akihiro Hachikubo received the B.S. degree in geophysics and the M.S. and Ph.D. degrees in environmental science from Hokkaido University, Sapporo, Japan.

He is currently an Associate Professor at the Kitami Institute of Technology, Kitami, Japan. His research interests are snow layer structure, thermal properties of deposited snow, and gas hydrates beneath the oceans and in permafrost regions.

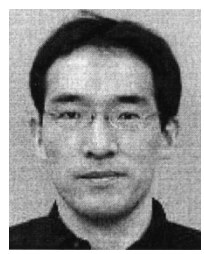

Masahiro Hori received the B.S., M.S., and Ph.D. degrees from the Hokkaido University, Sapporo, Japan, in 1993, 1995, and 1998, respectively.

He is currently an Engineer at the Earth Observation Research and Application Center, Japan Aerospace Exploration Agency, Tokyo. His area of research is optical remote sensing of snow, ice, and clouds.

Eleonora P. Zege received the B.S. degree in physics from the Belarussian State University, Minsk, Belarus, and the Ph.D. degree from the National Academy of Sciences of Belarus, Minsk, in 1959 and 1965, respectively.

She is currently the leader of the theoretical light scattering media optics group at the B. I. Stepanov Institute of Physics, Minsk. Her research interests are scalar and vector radiative transfer theory; imaging through scattering media; laser beam propagation and sounding; atmospheric and ocean optics; and satellite remote sensing of ocean, atmosphere, and cryosphere. She is the author of two books and more than 150 papers in refereed scientific journals.